Role of α-Helix Conformation Cooperating with NH···S Hydrogen Bond in the Active Site of Cytochrome P-450 and Chloroperoxidase: Synthesis and Properties of [M^{III}(OEP)(Cys-Helical Peptide)] (M = Fe and Ga)

Takafumi Ueno,[†] Yukihide Kousumi,[†] Kumiko Yoshizawa-Kumagaye,[‡] Kiichiro Nakajima,[‡] Norikazu Ueyama,*[,†] Taka-aki Okamura,[†] and Akira Nakamura*[,†]

Contribution from the Department of Macromolecular Science, Graduate School of Science, Osaka University, Toyonaka, Osaka 560-0043, Japan, and Peptide Institute, Inc., Minoh, Osaka 562-0015, Japan

Received January 2, 1998

Abstract: Heme-thiolate protein model complexes, [Fe^{III}(OEP)(Ac-L**c**XAF-LLLLL-ALFL-OMe)] {OEP = octhaethylporphinato, X = Leu (**1**) and Pro (**2**)}, having α-helical structure were synthesized and characterized as P-450 and CPO models. The stable ligation of cysteinyl thiolate at the axial position of model complexes was established using MCD, UV−visible, ^{1}H NMR, and ESI-MS. These results indicate that **1** and **2** possess high-spin 5-coordinated Fe(III) ions. The helical contents were examined by CD measurements in THF which revealed the contents of **1** and [Ga^{III}(OEP)(Ac-L**c**LAF-LLLLL-ALFL-OMe)] (**3**) to be both 49%, though the thiolate anion (Et_4N){Ac-LC(S^-)LAF-LLLLL-ALFL-OMe} (**5**) has the value of 57%. Thus, the α-helical NH···O═C hydrogen bond network is intercepted by the NH···S hydrogen bond between NH(Leu3) and S^γ(Cys2). However, the helical percentages of **2** (59%) and [Ga^{III}(OEP)(Ac-L**c**PAF-LLLLL-ALFL-OMe)] (**4**) (57%) are similar to that of (Et_4N){Ac-LC(S^-)LAF-LLLLL-ALFL-OMe} (**6**) (52%). The NMR analysis of the solution structure of the diamagnetic Ga(III) complex **4** indicates the distances between CysS^γ and NH of the third residue to be 2.37 Å, which is shorter than those of [Ga^{III}(OEP)(Z-**Cys**-Pro-Ala-Leu-OMe)] (2.58 Å) and [Ga^{III}(OEP)(Z-**Cys**-Pro-Leu-OMe)] (3.00 Å). These results show that the NH···S hydrogen bond of **4** is shortened by α-helix dipole and then the α-helix is stabilized. The redox potentials of Fe^{III}/Fe^{II} for **1** and **2** are −0.54 and −0.55 V (vs SCE in CH_2Cl_2), respectively. The values are more positively shifted from those of [Fe^{III}(OEP)(Z-**Cys**-Leu-Gly-OMe)] (−0.61 V vs SCE) and [Fe^{III}(OEP)(Z-**Cys**-Pro-Leu-OMe)] (−0.68 V vs SCE). Complex **1** indicates the positive shift of only 70 mV because the Cys-Leu-Ala fragment on the N terminus breaks the α-helical conformation. In contrast, complex **2** has larger positive shift (130 mV) by the α-helical conformation cooperating with the NH···S hydrogen bond. These data suggest that the redox reactions are regulated by the cooperating effect of the α-helix and the NH···S hydrogen bonds in the native enzymes.

Introduction

Heme-thiolate proteins are involved in a wide range of biological oxidations. P-450 catalyzes monooxygenation of a variety of hydrophobic organic substrates. CPO catalyzes halogenation reactions most often involving oxidation of the halide ion and formation of a C−X bond. The most distinctive feature in the structure of the enzyme is the coordination of a thiolate anion, from the proximal cysteine residue, to the heme iron as a fifth ligand.[1] A "consensus" mechanism has been proposed by the investigations of model complexes and native enzymes.[2] The role of the cysteinate proximal ligand of P-450 has been suggested a strong internal electron donor to promote O−O bond cleavage in the putative ferric-peroxide intermediate to generate the proposed ferryl-oxo "active oxygen" state of the reaction cycle.[2−5] Furthermore, the reduction from 5-coordinate high-spin Fe(III) to Fe(II), O_2 binding to the Fe(II) state, and the cleavage of the O−O bond in the catalytic cycle may be proceeded by the change of cysteinyl thiolate ligand basicity. As the model complexes of P-450s, a variety of aryl- and alkanethiolatoiron(III) (porphinato) complexes have been reported. Especially, it has been confirmed experimentally that an axial thiolate ligand of a P-450 model complex enhances heterolytic cleavage of the O−O bond on the iron porphyrin complex in hydrophobic media without the assistance of acid or base.[6] In the active centers of cytochrome P-450 and chloroperoxidase (CPO), the characteristic amino acid residues around the cysteine thiolate regulate chemical functions at some of the catalytic steps. Although the importance of such a cysteinyl ligand has been indicated by spectroscopic investiga-

* To whom correspondence should be addressed. Telephone: +81-6-850-5451. Fax: +81-6-850-5474. E-mail: ueyama@chem.sci.osaka-u.ac.jp, nakira.nakamura@nifty.ne.jp.

† Osaka University.

‡ Peptide Institute, Inc.

(1) *CYTOCHROME P450 Structure, Mechanism, and Biochemistry*; Ortiz de Montellano, P. R., Ed.; Plenum Press: New York, 1995.

(2) Dawson, J. H. *Science* **1988**, *240*, 435−439.

(3) Dawson, J. H.; Sono, M. *Chem. Rev.* **1987**, *87*, 1255−1276.

(4) Liu, H. I.; Sono, M.; Kadkhodayan, S.; Hager, L. P.; Hedman, B.; Hodgson, K. O.; Dawson, J. H. *J. Biol. Chem.* **1995**, *2270*, 10544−10550.

(5) Dawson, J. H.; Holm, R. H.; Trudell, J. R.; Barth, G.; Linder, R. E.; Bunnenberg, E.; Djerassi, C.; Tang, S. C. *J. Am. Chem. Soc.* **1976**, *98*, 3707−3709.

(6) Higuchi, T.; Shimada, K.; Maruyama, N.; Hirobe, M. *J. Am. Chem. Soc.* **1993**, *115*, 7551−7552.

10.1021/ja980016d CCC: $15.00
Published on Web 11/12/1998

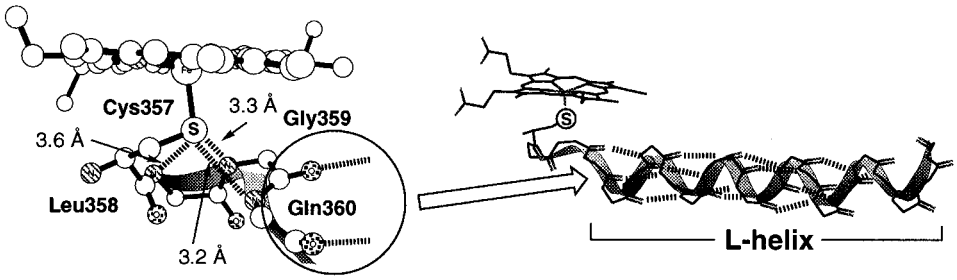

Figure 1. Close-up views of the heme thiolate active site and L-helix following the Cys357 of P-450cam.[16] Broad dashed lines indicate the hydrogen bonds. Boldface numbers show the distances between the cysteine sulfur and the nitrogen of peptide amide groups.

tions and reactions of the thiolate model complexes,[7−13] it has not been possible in these model studies to clarify variation of the cysteinyl basicity by the peptide conformation.

The crystal structures of heme-thiolate proteins have indicated some structural similarities.[14,15] The crystal structure analysis of P-450cam indicates that a hydrophobic environment called a "Cys pocket" exists around Cys357. The cysteinyl sulfur atom which is on the N terminus of the L-helix is suggested to form NH···S hydrogen bonds with the amide protons of Leu358, Gly359, and Gln360 (Figure 1).[16] Computational comparison among the three P-450s shows that the peptide conformation from the Cys pocket to the L-helix has the lowest root-mean-square deviation (rmsd) among the three crystal structures.[17] It is suggested that the NH···S hydrogen bond and the α-helix are both essential to regulate the Fe−S bond of P-450. CPO also has the NH···S hydrogen bonds and the cysteinyl residue on the N terminus of α-helix based on the X-ray crystal structural analysis.[18] Hence, the α-helical conformation cooperating with the invariant sequences, Cys-Leu-Gly-X (P-450) and Cys-Pro-Ala-Leu (CPO), is important to regulate the catalytic reaction of P-450 and CPO. In addition, nitrogenase[19] and thioredoxin[20] also have cysteinyl thiolates on the N terminus of α-helix. Kortemme et al. have reported that cysteinyl thiols on the N terminus of an α-helix have lower pK_a values.[21] Though it is estimated that such "active site helices" are significantly controlling the Fe−S bond of metalloenzymes,[18] the cooperative effect of the α-helix and the NH···S hydrogen bond to the heme-thiolate proteins has not been explained.

Therefore, we aimed at clarifying the cooperating effect of the α-helix and the NH···S hydrogen bond. We have already reported that the NH···S hydrogen bond makes positive shift of the Fe^{III}/Fe^{II} redox couple for the P-450 model complex, $[Fe^{III}(OEP)(S\text{-}2\text{-}CF_3CONHC_6H_4)]$.[10] In addition, it has been elucidated that the invariant sequences at the active sites, Cys-Leu-Gly-X (P-450) and Cys-Pro-Ala-Leu (CPO), keep the hairpin-turn conformations and then make the NH···S hydrogen bonds by our previous model investigation.[22] We report here the design, synthesis, spectroscopic characterization, electrochemical behavior, and solution structures in less polar solvent (THF, CH_2Cl_2, and $CHCl_3$) of a series of model complexes, $[M^{III}(OEP)$(cys-helical peptide)] (M = Fe and Ga), containing the invariant fragment and α-helical conformation.

Results

Design of α-Helical Peptides for the Model Complexes. The α-helix peptides were designed by references to the native sequences. The L-helix and the A-helix have been known to follow the cysteine residue in P-450s and CPO,[15] respectively, from the crystal structures of P-450s and CPO. From the structural comparison among P-450cam, P-450terp, and $P\text{-}450_{BM-3}$,[17] a high degree of sequence conservation extends from the invariant cysteine residue through most of the L-helix, which exhibits the lowest rmsd among the three structures. The primary sequences near the cysteinyl thiolate of P-450s and CPO were listed in Table 1.[17,23,24] The L-helix has 18 residues, and the percentage of hydrophobic residues is ca. 60%. In particular, leucine residues predominate (40%). The A-helix of CPO consists of 10 amino acid residues, and the percentage of hydrophobic residues is also ca. 60%.

The model peptides were used to elucidate the role of the α-helical cysteine thiolate complexes where the cysteine residue is located at the N terminus of the α-helix. These models were designed to meet several criteria: (1) The peptides should form stable α-helix conformations in less polar solvent (THF, CH_2Cl_2, and $CHCl_3$) for characterization and synthesis of the Fe(III) and Ga(III) model complexes and the corresponding cysteinyl thiolate anion peptides. Our peptide design is based on the propensity of leucine residue to prefer high ability of helix formation[25,26] and solubility in organic solvents.[27] (2) The peptides should contain the invariant fragments of P-450 and of CPO (Table 1). As a P-450 model, an Ac-Leu-Cys-Leu-Ala fragment was introduced on the N terminus of the model peptide. The glycine following the -Cys-Leu- fragment in P-450

(7) Stäubli, B.; Fretz, H.; Piantini, U.; Woggon, W.-D. *Helv. Chimi. Acta* **1987**, *70*, 1173−1193.
(8) Tang, S. C.; Koch, S.; Papaefthymiou, G. C.; Foner, S.; Frankel, R. B.; Ibers, J. A.; Holm, R. H. *J. Am. Chem. Soc.* **1976**, *98*, 2414−2434.
(9) Wagenknecht, H.-A.; Woggon, W.-D. *Angew. Chem., Int. Ed. Engl.* **1997**, *36*, 390−392.
(10) Ueyama, N.; Nishikawa, N.; Yamada, Y.; Okamura, T.; Nakamura, A. *J. Am. Chem. Soc.* **1996**, *118*, 12826−12827.
(11) Ogoshi, H.; Sugimoto, H.; Yoshida, Z. *Tetrahedron Lett.* **1975**, *27*, 2289−2292.
(12) Schappacher, M.; Richard, L.; Fischer, J.; Weiss, R.; Bill, E.; Montiel-Montoya, R.; Winkler, H.; Trautwein, A. X. *Eur. J. Biochem.* **1987**, *168*, 419−429.
(13) Schappacher, M.; Richard, L.; Fischer, J.; Weiss, R.; Montiel-Montoya, R.; Bill, E.; Trautwein, A. X. *Inorg. Chem.* **1989**, *28*, 4639−4645.
(14) Poulos, T. L.; Finzel, B. C.; Howard, A. J. *J. Mol. Biol.* **1987**, *195*, 687−700.
(15) Sundaramoorthy, M.; Terner, J.; Poulos, T. L. *Structure* **1995**, *3*, 1367−1377.
(16) Raag, R.; Poulos, T. L. *Biochemistry* **1989**, *28*, 917−922.
(17) Hasemann, C. A.; Kurumbail, R. G.; Boddupalli, S. S.; Peterson, J. A.; Deisenhofer, J. *Structure* **1995**, *2*, 41−62.
(18) Poulos, T. L. *JBIC, J. Biol. Inorg. Chem.* **1996**, *1*, 356−359.
(19) Kim, J.; Woo, D.; Rees, D. C. *Biochemistry* **1993**, *32*, 7104−7115.
(20) Hol, W. G. J. *Prog. Biophys. Mol. Biol.* **1985**, *45*, 149−195.
(21) Kortemme, T.; Creighton, T. E. *J. Mol. Biol.* **1995**, *253*, 799−812.
(22) Ueno, T.; Nishikawa, N.; Moriyama, S.; Ueyama, N.; Nakamura, A. Submitted to *Inorg. Chem.*
(23) Cupp-Vickery, J. R.; Poulos, T. L. *Nat. Struct. Biol.* **1995**, *2*, 144−153.
(24) Keningsberg, P.; Fang, G.-H.; Hager, L. P. *Arch. Biochem. Biophys.* **1987**, *254*, 409−415.
(25) Gans, P. J.; Lyu, P. C.; Manning, M. C.; Woody, R. W. *Biopolymers* **1991**, *31*.
(26) Richardson, J. S.; Richardson, D. C. *Scienec* **1988**, *240*, 1648−1652.
(27) Narita, M.; Kojima, Y.; Isokawa, S. *Bull. Chem. Soc. Jpn.* **1989**, *62*, 1976−1981.

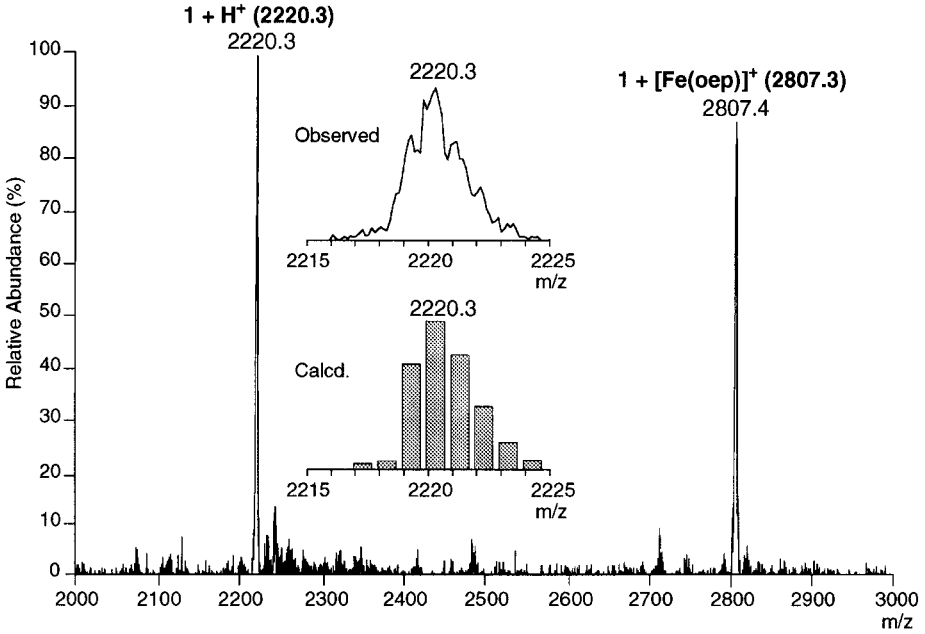

Figure 2. Electrospray ionization mass spectrum of complex **1** (positive ionization mode) in acetonitrile/dichloromethane (1:1) (0.1 mM).

(Table 1) is substituted by Ala because of the peptide solubility. The CPO model peptide contains Ac-Leu-Cys-Pro-Ala at the N terminus. The Ac-Leu was adopted as the N terminus blocking fragment in these sequences because each of P-450cam and CPO has a hydrophobic residue, Leu (P-450cam) or Pro (CPO), at the N terminus of the cysteine residue (Table 1). (3) The details of the solution structures should be investigated by ^{1}H NMR spectroscopy. We employed the peptides having 14 amino acid residues containing Phe and Ala residues to assign the peaks easily by COSY, TOCSY, and ROESY. To satisfy all of the above conditions, the sequences of the peptides investigated here are Ac-LCLAF-LLLLL-ALFL-OMe and Ac-LCPAF-LLLLL-ALFL-OMe. They are adopted as the model helical ligands of P-450 and CPO, respectively.

Synthesis of [M^{III}(OEP)(Cys-Helical Peptide)] Complexes (M = Fe and Ga). Complexes **1** and **2** were synthesized by the ligand exchange reaction between [Fe^{III}(OEP)(OMe)] and the corresponding peptide ligand.[22] The reasons for use of octaethyl porphyrin were already described in our previous paper.[22] The reaction products were characterized by a combination of spectroscopic methods. The ^{1}H NMR data show that the ligand exchange reaction proceeded completely. ESI-MS data for complexes **1** and **2** indicate the 5-coordinate Fe(III) with the composition [Fe^{III}(OEP)(Cys-helical peptide)] (see the Experimental Section and Figure 2). The peptide sequences remarkably contribute thermal stability of the peptide complexes. Thus, the Fe(III) complexes containing the invariant fragments of P-450 and CPO are thermally stable at 30 °C in CH_2Cl_2 as reported for the tetra- and tripeptide complexes containing the NH···S hydrogen bond.[22] The thermal stabilities of **1** and **2** are higher than those of dipeptide complexes[22] because the α-helix decreases the pK_a value of the cysteinyl thiol at the N terminus.[21] Ga(III) peptide complexes [Ga^{III}(OEP)(Cys-helical peptide)] were also synthesized by the reported ligand exchange reaction.[22] The structure of the 5-coordinate Ga(III) peptide complexes were confirmed by the ^{1}H NMR integral ratio between the porphyrin and the peptide signals (data not shown) and also by ESI-MS (see the Experimental Section). We also examined reduction of the high-spin Fe(III) complexes to the Fe(II)(CO) complexes using (n-Bu)$_4$NBH$_4$ in CH_2Cl_2 under a CO atmosphere. The expected carbonyl, [Fe^{II}(CO)(OEP)(Z-**Cys**-Pro-Ala-Leu-OMe)], was confirmed by ^{1}H NMR and UV−vis spectroscopy, but the reduction of [Fe^{III}(OEP)(Z-**Cys**-Leu-Gly-Leu-OMe)] and the α-helix complexes, **1** and **2,** was unsuccessful.

Table 1. Multiple Sequence Alignment of Various P-450s[a] and CPO[b] Primarily Based on Sequence Conservation

	Cys pocket		L-helix
	530	540	550
P450cam	H**G**SHL**C**L**G**QH	LARREIIVTL	KEWLTRIP..
P450terp	W**G**AHM**C**L**G**QH	LAKLEMKIFF	EELLPKLK..
P450BM3	N**G**QRA**C**I**G**QQ	FALHEATLVL	GMMLKHFDF.
P450eryF	Q**G**IHF**C**M**G**RP	LAKLEGEVAL	RALFGRFP..
P450scc	W**G**VRQ**C**V**G**RR	IAELEMTLFL	IHILENFKV.
P45026-ohp	Y**G**VRA**C**L**G**RR	IAELEMQLLL	ARLIQRYEL.
P450c21B	C**G**APV**C**L**G**EP	LARLELFVVL	TRLLQAFTLL
P45017a	A**G**PRS**C**I**G**EA	LARQELFVFT	ALLLQRFDL.
P450d	L**G**KRR**C**I**G**EI	PAKWEVFLFL	AILLHQLEF.
P450M1	A**G**KRI**C**A**G**EA	LARTELFLFF	TTILQNFNL.
P450PBc4	A**G**KRMCVGEG	LARMELFLFL	TSILQNFKL.
P4503a	A**G**KRV**C**V**G**EG	LARMELFLLL	SAILOHFNL.
P450b	T**G**KRI**C**L**G**EG	IARNELFLFF	TTILQNFSV.
P45015aoh-1	I**G**KRY**C**F**G**EG	LARMELFLFL	TNIMQNFHF.
P450nf-25	S**G**PRN**C**I**G**MR	FALMNMKLAL	IRVLQNFSF.
P450Arom	F**G**PRG**C**A**G**KY	IAMVMMKAIL	VTLLRRFHVK
CPO	DSRAP**C**PALNA-LANHGYI		

[a] References 17 and 23. [b] Reference 24.

Electronic and Magnetic Circular Dichroism Spectra. The electronic spectral data for [Fe^{III}(OEP)(Cys-peptide)] complexes are summarized in Table 2, and the spectra of the complexes in dichloromethane are shown in Figure 3. Each spectrum consists of an α band near 635 nm, a broad absorption in the β band region containing a shoulder superimposed on a maximum at 505−533 nm, and a Soret band at ca. 370 nm. Thus, all of the spectra are clearly of the high-spin type.[8,11,22,28]

The MCD spectra of the model complexes are shown in Figure 3, and the MCD spectral data are listed in Table 3. MCD spectroscopy has already been utilized to probe the structure of the high-spin ferric states of these two enzymes.[5,29,30] The most important feature of these spectra is the strong negative absorption in the Soret region (ca. 400 nm) common to the

(28) Uno, T.; Hatano, K.; Nishimura, Y.; Arata, Y. *Inorg. Chem.* **1990**, *29*, 2803−2807.

Table 2. Electronic Spectral Data[a] for [Fe^{III}(OEP)(Cys-Helical Peptide)] Complexes

complexes	λ_{max} nm (ϵ, mM^{-1} cm^{-1}) α	β		Soret
[Fe^{III}(OEP(Ac-L**c**LAF-LLLLL-ALFLOMe)] (**1**)	635 (4.5)	533 (10.0)	505 (10.4)	373 (88.4)
[Fe^{III}(OEP(Ac-L**c**PAF-LLLLL-ALFLOMe)] (**2**)	637 (4.1)	531 (9.2)	508 (9.7)	371 (82.2)
[Fe^{III}(OEP)(Z-**Cys**-Leu-Gly-Leu-OMe)][b]	635 (5.6)	529 (10.9)	506 (11.7)	373 (96.9)
[Fe^{III}(OEP)(Z-**Cys**-Leu-Gly-OMe)][b]	635 (4.3)	530 (8.6)	505 (9.2)	373 (76.6)
[Fe^{III}(OEP)(Z-**Cys**-Pro-Ala-Leu-OMe)][b]	637 (4.2)	533 (8.4)	506 (8.8)	372 (73.0)
[Fe^{III}(OEP)(Z-**Cys**-Pro-Leu-Ala-OMe)][b]	635 (5.7)	532 (11.5)	506 (11.9)	370 (98.9)
[Fe^{III}(OEP)(Z-**Cys**-Pro-Leu-OMe)][b]	631 (4.2)	533 (8.2)	505 (9.2)	373 (71.5)

[a] In dichloromethane at 30 °C (0.2 mM). [b] Reference 22.

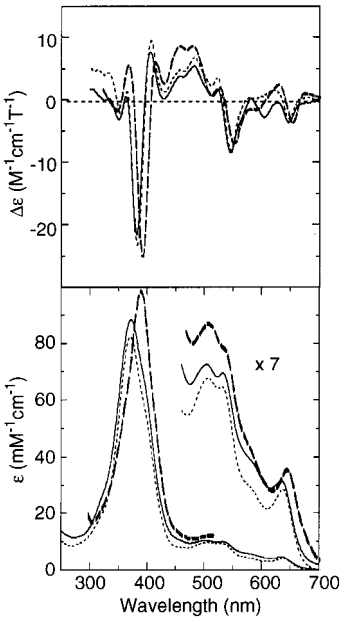

Figure 3. (a) MCD and (b) UV−visible spectra of [Fe^{III}(OEP)(Ac-L**c**LAF-LLLLL-ALFL-OMe)] (**1**) (—), [Fe^{III}(OEP)(Ac-L**c**PAF-LLLLL-ALFL-OMe)] (**2**) (- - -) in dichloromethane, and P-450cam (high-spin 5-coordinate ferric iron) (— — —).[5,30] The spectra were measured in CH_2Cl_2 (0.2 mM) at room temperature.

peptide model complexes and the native enzymes. The MCD spectra also ensure that complexes **1** and **2** have a high-spin 5-coordinate Fe(III) state.

CD Studies. The CD spectra are shown in Figure 4. Tetrahydrofuran was employed for CD measurements because the complexes are highly soluble in the solvent (less soluble in acetonitrile) and the solvent cannot ligate to the metal ion at 27 °C.[8,31] Complexes **1**−**4** show negative bands corresponding to the amide n−π* transition in the vicinity of 220−222 nm and negative bands near 208 nm. The two characteristic minima indicate the peptides to be predominantly in α-helical conformation.[32] The ellipticity at 222 nm is the most commonly used parameter to describe α-helical conformation. The calculated values of percent helicity from $[\theta]_{222}$ (evaluated by per-residue molar ellipticity at 222 nm) are reported in Table 4. Complexes **2** differs from **1** only in the proline substitution for the leucine residue next to the cysteine residue. Complex **1** (49%) has a lower helical content than **2** (59%), though the helical propensity of proline residue is much lower that of leucine. This suggests

Table 3. MCD Spectral Data[a] for [Fe^{III}(OEP)(Cys-Helical Peptide)] Complexes

complexes	λ_{max} nm ($\Delta\epsilon$/H M^{-1} cm^{-1} T^{-1})
[Fe^{III}(OEP(Ac-L**c**LAF-LLLLL-ALFLOMe)] (**1**)	350.2 (−3.15), 381.6 (−21.59), 405.4 (7.67), 482 (5.45), 545.8 (−8.52), 604.2 (−2.84), 646.6 (−3.65)
[Fe^{III}(OEP(Ac-L**c**PAF-LLLLL-ALFLOMe)] (**2**)	354 (−2.40), 382.6 (−23.28), 406.4 (9.36), 482.8 (6.77), 546.2 (−8.12), 619.8 (1.49), 647 (−3.07)
[Fe^{III}(OEP)(Z-**Cys**-Leu-Gly-Leu-OMe)][b]	300.5 (3.8), 333.5 (2.7), 351 (−1.0), 364 (4.5), 383 (−25.9), 407 (9.7), 481.5 (7.7), 522.5 (3.23), 546 (−9.4), 595.5 (−0.7), 622.5 (1.6), 646 (−3.4)
[Fe^{III}(OEP)(Z-**Cys**-Leu-Gly-OMe)][b]	299.5 (3.4), 350 (−0.8), 364 (3.8), 382.5 (−17.8), 406.5 (6.9), 481 (5.4), 522.5 (2.3), 545.5 (−7.1), 580 (0.4), 604 (−1.5), 624 (0.6), 645.5 (−2.8), 680.5 (0.3)
[Fe^{III}(OEP)(Z-**Cys**-Pro-Ala-Leu-OMe)][b]	305.0 (3.7), 351.5 (−1.8), 363.5 (2.1), 383.0 (−22.6), 406.5 (8.0), 480.5 (5.0), 521.0 (1.6), 544.0 (−8.7), 621,5 (1.0), 644.5 (−3.2)
[Fe^{III}(OEP)(Z-**Cys**-Pro-Leu-Ala-OMe)][b]	383.8 (−15.1), 406.8 (8.2), 483.6 (6.9), 547 (−10.4), 621.8 (1.4), 648.2 (−3.3)
[Fe^{III}(OEP)(Z-**Cys**-Pro-Leu-OMe)][b]	301.5 (3.5), 329 (3.6), 349.5 (−0.4), 362.5 (3.0), 382.5 (−16.6), 406.5 (6.0), 481 (5.1), 522 (2.1), 545.5 (−6.2), 581.5 (0.8), 604 (−1.1), 624 (0.9), 646 (−2.4)

[a] In dichloromethane (0.2 mM) at ambient temperature. [b] Reference 22.

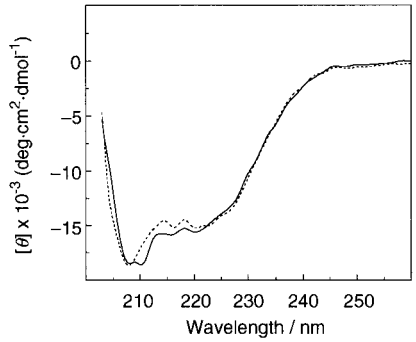

Figure 4. CD spectra of [Fe^{III}(OEP)(Ac-L**c**LAF-LLLLL-ALFL-OMe)] (**1**) (solid line) and [Ga^{III}(OEP)(Ac-L**c**LAF-LLLLL-ALFL-OMe)] (**3**) (dotted line) in THF at 27 °C (0.5 mM).

a cooperative effect of proline and cysteine on the helix stability. The corresponding Ga(III) complexes have helical conformations similar to those of the Fe(III) complexes because **3** and **4** indicate quite helical contents similar to those of **1** and **2**, respectively. A little increase of helicity for **1**−**4** compared with the corresponding helical peptides indicates that the α-helical structures of the peptide ligand can be slightly more stabilized by the presence of the metalloporphyrin. On the other hand, the cysteinyl thiolate anions, **5** and **6,** disturb α-helical conformation. The thiolate anion **5** has a more stable α-helix than the corresponding thiol peptide (44%) and complexes **1**

(29) Dawson, J. H.; Trudell, J. R.; Barth, G.; Linder, R. E.; Bunnenberg, E.; Djerassi, C.; Chiang, R.; Hanger, L. P. *J. Am. Chem. Soc.* **1976**, *98*, 3709−3710.
(30) Sono, M.; Stuehr, D. J.; Ikeda-Saito, M.; Dawson, J. H. *J. Biol. Chem.* **1995**, *270*, 19943−19948.
(31) Collman, J. P.; Sorrell, T. N.; Hoffman, B. M. *J. Am. Chem. Soc.* **1975**, *97*, 913−914.
(32) Greenfield, N.; Fasman, G. D. *Biochemistry* **1969**, *8*, 4108−4116.

Table 4. $[\theta]_{222}$ Values and Percentage of Helical Content of Fe(III) and Ga(III) Complexes in Tetrahydrofuran at 27 °C (0.5 mM)

complexes	$[\theta]_{222}$	helical content (%)[b]
[Fe^{III}(OEP)(Ac-L**c**LAF-LLLLL-ALFL-OMe)] (**1**)	−15200	49
[Fe^{III}(OEP)(Ac-L**c**PAF-LLLLL-ALFL-OMe)] (**2**)	−17900	59
[Ga^{III}(OEP)(Ac-L**c**LAF-LLLLL-ALFL-OMe)] (**3**)	−15000	49
[Ga^{III}(OEP)(Ac-L**c**PAF-LLLLL-ALFL-OMe)] (**4**)	−17400	57
Ac-LCLAF-LLLLL-ALFL-OMe[a]	−13500	44
Ac-LCPAF-LLLLL-ALFL-OMe[a]	−15900	52
(Et_4N){Ac-LC(S^-)LAF-LLLLL-ALFL-OMe} (**5**)[a]	−17300	57
(Et_4N){Ac-LC(S^-)PAF-LLLLL-ALFL-OMe} (**6**)[a]	−16000	52

[a] Conditions; 1.0 mM in THF at 27 °C. [b] Calculated from ratio the $([\theta]_{222} - [\Theta]_U)/([\Theta]_H - [\Theta]_U)$, where the values $[\Theta]_H$ and $[\Theta]_U$ are the signals for 100 and 0% helix, respectively. $[\Theta]_H$ and $[\Theta]_U$ can be estimated at various temperatures, t in °C, from $[\Theta]_H = -40\,000(1 - 2.5/n)$ deg cm^2 dmol^{-1} + 100t (n = 14) and $[\Theta]_U = +640 - 45t$, respectively.[70,71]

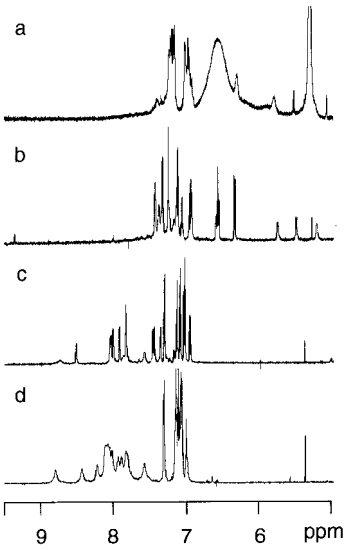

Figure 5. ^{1}H NMR spectra of (a) [Fe^{III}(OEP)(Ac-L**c**PAF-LLLLL-ALFL-OMe)] (**2**) in CD_2Cl_2 at 30 °C (400 MHz), (b) [Ga^{III}(OEP)(Ac-L**c**PAF-LLLLL-ALFL-OMe)] (**4**) in $CDCl_3$ at 27 °C (600 MHz), (c) (Et_4N){Ac-LC(S^-)PAF-LLLLL-ALFL-OMe}, and (d) Ac-LCPAF-LLLLL-ALFL-OMe in THF-d_8 at 27 °C (600 MHz).[40] The concentration of these samples is 2.0 mM.

(49%). But **6** has a smaller α-helical content than **2** and **4**. Thus, not only the identity of the residue following the cysteine residue but also the state of cysteine residue, i.e., −SH, $-S^-$, and −S−M(por), is important to regulate their conformation.

^{1}H NMR Studies. NMR Chemical Shifts. ^{1}H NMR spectra of complexes **2**, **4**, the corresponding cysteinyl thiol and thiolate anion helical peptides are shown in Figure 5. Complexes **1** and **2** have the meso, α-H, and β-H resonances at ca. −45, +40, and +6 ppm, respectively. All of the present Fe(III) helical peptide complexes have ^{1}H NMR chemical shifts of the OEP rings similar to those of the reported high-spin 5-coordinated Fe(III) thiolate complexes.[22,33,34] Except for the protons of the OEP, no signals are observed between +400 and −100 ppm. Thus, the peaks between +80 and +40 ppm may be assigned as the protons of amino acid residues close to the distal site of P-450 and CPO.[35] With respect to the signals of the axial cysteinate protons, the CysC_β protons of native high-spin ferric P-450 and CPO are not detectable due to the larger shift and line broadening.[35,36] Because **1** and **2** also have the same problem, our paramagnetic complexes do not allow ^{1}H NMR solution structural characterization. The investigation of their ^{13}C,^{15}N labeled samples remains as an important future problem.

The ^{1}H NMR resonance assignments for **4** at 27 °C in $CDCl_3$ are presented in Table 5. However, complete assignments for **3** were impossible due to severe overlap in the ROESY spectra. Although the NMR spectra of high-spin Fe(III) complexes feature large line width and poor spectral resolution, the diamagnetic gallium complexes displayed spectra in a much narrower line width (Figure 5). The OEP ligand has been adopted because of its good separation of the proton peaks of the peptide from the peaks of the porphyrin protons (Table 5). In addition, the two-dimensional experiments for the gallium complexes were carried out by the standard methods[37,38] because the Ga(III) complexes lack protons having very short T_1 value (Figure 6).[22] The assignment of most of the resonance was greatly aided by comparison with the spectrum of [Ga^{III}(OEP)(Cys-peptide)], whose resonances had been previously assigned.[22]

Various features in ^{1}H NMR can be observed for the diamagnetic Ga(III) complex **4**. Of primary interest are the large upfield shifts experienced by the protons of peptide ligands coordinated to the Ga(III) ion (Figure 5). The space directly above the center of the porphyrin ring should provide the greatest shielding by ring current effect.[39] For example, the resonances of side chain protons of Cys2, Pro3, and Ala4 are shifted to upfield compared to those of the corresponding cysteinyl thiolate anion helical peptide[40] by the ring current effect. Especially, the observed ring current shifts of Pro3C^δ (−0.96 and −3.12 ppm) and Ala4C^β (−2.01 ppm) are larger than those of the other side chains.

The thiol peptides have the broad signals caused by aggregation, but the corresponding thiolate anion peptides have separate signals at the NH region under the condition as shown in Figure 5. In addition, the cysteinyl amide protons of **5** and **6** are observed at 10.14 and 10.64 ppm, respectively.[40] The observed lowfield shift is induced by an intraresidue NH···S hydrogen bond.[41]

Coupling Constants and Temperature Coefficients. The coupling constants and the temperature coefficients measured for **4** also strongly suggest some kinds of helical conformation. Coupling constants measured for **4** at 27 °C show values of $^3J_{HN\alpha} = 3.5-5.5$ Hz each from Ala4 to Leu12, consistent with a ϕ angle in a helical dihedral space ($\phi \leq -70°$).[42] The temperature dependence of the amide proton chemical shift is an indication of possible intramolecular hydrogen bonding and, as such, can be an indication of the formation of an α-helix. For oligopeptides in $CDCl_3$, the temperature coefficients of the amide proton resonances are expected to be $-\Delta\delta/\Delta T \geq 3.2$ ppb K^{-1}, when intermolecular self-association is significant or

(33) Ueyama, N.; Nishikawa, N.; Okamura, T.; Yamada, Y.; Nakamura, A. *Inorg. Chem.* **1998**, *37*, 2415.
(34) Arasasingham, R. D.; Balch, A. L.; Cornman, C. R.; Ropp, J. S. d.; Eguchi, K.; LaMar, G. N. *Inorg. Chem.* **1990**, *29*, 1847−1850.
(35) Lukat, G. S.; Goff, H. M. *Biochim. Biophys. Acta* **1990**, *1037*, 351−359.
(36) Bertini, I.; Turano, P.; Vila, A. J. *Chem. Rev.* **1993**, *93*, 2833−2932.
(37) Wüthrich, K. *NMR of Proteins and Nucleic Acids*; Wiley: New York, 1986.
(38) Vo, E.; Wang, H. C.; Germanas, J. P. *J. Am. Chem. Soc.* **1997**, *119*, 1934−1940.
(39) Janson, T. R.; Katz, J. J. *The Porphyrins*; Dolphin, D., Ed.; Academic Press: New York, 1979; Vol. IV, pp 1−59.
(40) See the Supporting Information.
(41) Ueyama, N.; Moriyama, S.; Ueno, T.; Nakamura, A. *Pept. Chem.* **1998**, in press.
(42) Paradi, A.; Billeter, M.; Wüthrich, K. *J. Mol. Biol.* **1984**, *180*, 741−751.

Table 5. ^{1}H NMR Chemical Shifts for [Ga^{III}(OEP)(Ac-LcPAF-L$_5$-ALFL-OMe)] in $CDCl_3$ at 27 °C (2.0 mM)

residues	NH ($^3J_{HN\alpha}$/Hz)	$\Delta\delta/\Delta T$ (ppb/K)	αH	βH	γH	other
Leu1	5.506 (7.1)	−0.23	3.945	1.201, 1.160	1.341	δH 0.720, 0.699
Cys2	4.642 (7.3)	3.5	1.198	−3.414, −1.121		
Pro3			3.386	1.880, 1.398	1.699, 1.230	δH 2.558, 0.399
Ala4	5.223 (4.0)	0.69	3.177	−0.566		
Phe5	5.757 (3.7)	1.33	3.515	2.363, 2.067		2,6H 6.346, 3,5H 6.576, 4H 6.967
Leu6	6.611 (4.6)	2.83	3.644	1.374, 1.333	1.316	δH 0.666, 0.646
Leu7	6.948 (4.9)	3.15	3.821	1.559, 1.436	1.555	δH 0.783, 0.824
Leu8	6.954 (4.9)	2.63	3.883	1.518, 1.473	1.526	δH 0.742
Leu9	7.162 (5.5)	3.13	3.887	1.658, 1.497	1.691	δH 0.790, 0.7369
Leu10	7.442 (4.3)	2.91	4.027	1.756, 1.604	1.752	δH 0.851, 0.814
Ala11	7.450 (3.7)	2.62	3.998	1.466		
Leu12	7.248 (5.2)	3.66	4.089	1.571, 1.292	1.559	δH 0.729, 0.775
Phe13	7.389 (8.3)	2.07	4.633	3.437, 2.915		2,6H 7.337, 3,5H 7.134, 4H 7.069
Leu14	7.360 (8.0)	3.11	4.533	1.810, 1.637	1.797	δH 0.905
Ac						1.552
OMe						3.675
meso (OEP)						10.370
CH_3 (OEP)						1.968
CH_2 (OEP)						4.247, 4.152

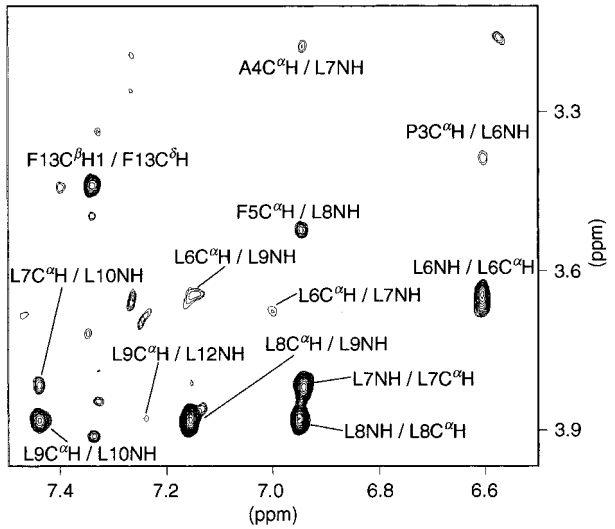

Figure 6. $d_{\alpha N}$ region of the 600-MHz ROESY spectrum of [Ga^{III}(OEP)-(Ac-L**c**PAF-LLLLL-ALFL-OMe)] (**4**) in $CDCl_3$ at 27 °C (2.0 mM). A 200-ms mixing time was used.

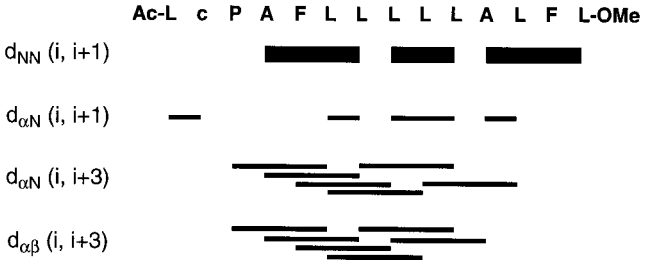

Figure 7. Schematic diagram showing the magnitude of various ROE connectivities observed in the ROESY spectrum for **4** in $CDCl_3$ at 27 °C (mixing time = 200 ms).

when intramolecularly hydrogen-bonded conformations unfold as the temperature is increased, whereas for protected (hydrogen bonded or buried) amides, these values are expected to decrease to $-\Delta\delta/\Delta T \leq 3.2$ ppb K^{-1}.[43,44] The temperature coefficients for the amide backbone protons of **4** are listed in Table 5. They show values of $-\Delta\delta/\Delta T \leq 3.2$ ppb K^{-1}, except for Cys2 and Leu12 NHs, consistent with the involvement of these amides in the intramolecular hydrogen bonds present in the α-helix without aggregation.

For **5** and **6**, $^3J_{HN\alpha}$ values from Phe5 to Ala11 are below 5 Hz[40] and the temperature coefficients indicate that they have intramolecular hydrogen bonds except for Leu3 ($-\Delta\delta/\Delta T$ = 11.7) of **5**. These data show the α-helical conformation of **5** and **6**. The Leu3 amide proton of **5** probably has some intermolecular interactions at low temperature.

ROESY Connectivities. ROE connectivities diagnostic of α-helix include a series of relatively strong $d_{NN}(i, i+1)$ connectivities, accompanied by $d_{\alpha N}(i, i+1)$, $d_{\alpha N}(i, i+3)$, and $d_{\alpha\beta}(i, i+3)$ ROEs.[37] Figure 6 shows the $d_{\alpha N}$ region of the 600-MHz ROESY (mixing time = 200 ms) spectrum of **4** at 27 °C in $CDCl_3$. Figure 7 is a schematic diagram showing the magnitude of the various ROE connectivities observed in the ROESY spectrum of **4**. ROE connectivities of $d_{NN}(i, i+1)$, $d_{\alpha N}(i, i+1)$, $d_{\alpha N}(i, i+3)$, and $d_{\alpha\beta}(i, i+3)$ observed from the N-terminus to the C-terminus of **4** clearly demonstrate that the peptide is in a helical conformation throughout its length. ROEs of $d_{\alpha N}(i, i+2)$ were not observed for **4** (Figure 7) though the 3_{10}-helix generally displays $d_{\alpha N}(i, i+2)$ ROEs which are not observed for the α-helix.[37] Thus, these data suggest that **4** has α-helical character in $CDCl_3$ at 27 °C. In addition, a strong ROE between Cys C$^\alpha$H and Pro C$^\delta$ protons shows that the peptide bond of the Cys-Pro has kept a trans conformation.[45] The corresponding thiolate anion peptides **5** and **6** also indicate α-helical ROE connectivities.[40]

Restricted Molecular Mechanics (rMM) and Restrained Molecular Dynamics (rMD) Structure Calculations of [Ga^{III}-(OEP)(Ac-LcLPAF-LLLLL-ALFL-OMe)] (4). Interproton distance restraints (70 intraresidue ROEs and 36 interresidue ROEs) were generated from the ROESY data and were used as a basis for calculating a structure for **4**. We employed the backbone NH(i)···O=C(i+4) (i = 1−10) hydrogen bond constraints provided by the temperature dependence of the NH chemical shifts (Table 5). A hydrogen bond restrain between NH of Ala4 and Sγ of Cys2 is not used for these calculations. Though structural calculations without the inclusion of the backbone NH···O=C restraints were performed, the generated structures do not satisfy the experimental data (root-mean-square violation, $rms_{viol} > 0.25$). The dihedral angle restraints based on the observed $^3J_{HN\alpha}$ were not utilized. A total of 50 structures

(43) Stevens, E. S.; Sugawara, N.; Bonora, G. M.; Toniolo, C. *J. Am. Chem. Soc.* **1980**, *102*, 7048−7050.

(44) Pease, L. G.; Watson, C. *J. Am. Chem. Soc.* **1978**, *100*, 1279−1286.

(45) Wüthrich, K.; Braun, M. B. W. *J. Mol. Biol.* **1984**, *180*, 715−740.

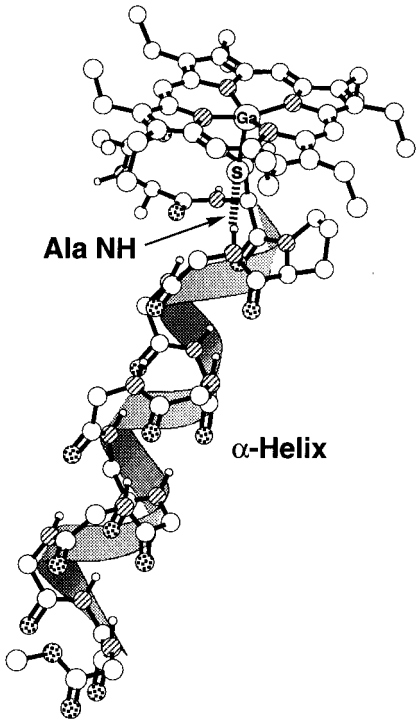

Figure 8. rMM and rMD structure of [Ga^{III}(OEP)(Ac-L**c**PAF-LLLLL-ALFL-OMe)] (**4**).

was generated (details are described in the Experimental Section). A rms_{viol} of 0.20 Å is the lowest value among the 50 structures. The conformational family to perform the structural analysis consists of 17 structures whose backbone heavy atoms of residues Leu1 to Leu14 are well defined (average rmsd from the lowest rms_{viol} structure, 0.32 ± 0.12 Å). The structures agree with the input data very well, with no rms_{viol}'s above 0.25 Å. The averaged structure of the conformational family was used for the calculations for Ga(III) complex **4**.

Figure 8 shows the rMM- and rMD-calculated structure of **4** using the ESFF force field.[46] The Ga−S−C angle of the calculated structure is 107.5°, which is similar to that of CPO (110.5°).[15] Interestingly, the distance between Ala4 N and Cys2 S^{γ} is 3.30 Å in the structure, indicating that an NH···S hydrogen bond interaction also exists in the α-helical peptide as reported for metalloproteins[15,47] and model complexes.[22,33,48] The absence of the hydrogen bond is inferred from the distance between Leu5 N and Cys2 S^{γ} (4.93 Å) because the amide proton forms the NH···O═C hydrogen bond with Leu1 C═O (N···O = 3.05 Å). Hydrogen-bonding interactions confirmed both by the calculated structure of **4** and the temperature coefficients (Table 5) also support an α-helical structure for **4**. NH(*i*)-O(*i* − 4) hydrogen bonds are observed for the amide protons of Leu6−Leu13. The backbone dihedral angles from Ala4 to Ala11 are close to those expected for an ideal α-helix (mean $\phi = -62°$, mean $\psi = -41°$). ψ angles of Leu12, Phe13, and Leu14 are higher than ideal (mean 72°). In addition, the dihedral angles in Leu1−Pro3 region, ϕ and ψ, are deviated from the regular helical angles because of the specific hydrogen bonding. Thus, the ^{1}H NMR data indicate that the α-helical solution structure for **4** keeps the NH···S hydrogen bond on the N terminus.

(46) *Insight II User Guide, October 1995*; Biosym/MSI: San Diego, CA, 1995.

(47) Adman, E.; Watenpaugh, K. D.; Jensen, L. H. *Proc. Natl. Acad. Sci. U.S.A.* **1975**, *72*, 4854−4858.

(48) Ueyama, N.; Okamura, T.; Nakamura, A. *J. Chem. Soc., Chem. Commun.* **1992**, 1019−1020.

Table 6. Redox Potentials of Fe^{III}/Fe^{II} for [Fe^{III}(OEP)(Cys-Helical Peptide)] in Dichloromethane[a]

complexes	$E_{1/2}$,[b] V (i_{pa}/i_{pc})
[Fe^{III}(OEP)(Ac-L**c**LAF-LLLLL-ALFLOMe)] (**1**)	−0.54 (0.8)
[Fe^{III}(OEP)(Ac-L**c**PAF-LLLLL-ALFLOMe)] (**2**)	−0.55 (0.7)
[Fe^{III}(OEP)(Z-**Cys**-Leu-Gly-Leu-OMe)][b]	−0.59 (0.9)
[Fe^{III}(OEP)(Z-**Cys**-Pro-Ala-Leu-OMe)][b]	−0.65 (0.8)
[Fe^{III}(OEP)(Z-**Cys**-Leu-Gly-OMe)][b]	−0.61 (0.7)
[Fe^{III}(OEP)(Z-**Cys**-Pro-Leu-OMe)][b]	−0.68 (0.9)
P-450cam (substrate binding)[c]	−0.42

[a] Concentration of the sample was 2 mM, containing 200 mM of *n*-Bu_4NClO_4 as a supporting electrolyte. The scan rate was 100 mV/s. [b] vs SCE. Reference 22. [c] Reference 55.

Electrochemical Property. Table 6 lists Fe^{III}/Fe^{II} redox potentials for various Fe(III) Cys-containing peptide complexes. Complex **1** has the positive shifted Fe^{III}/Fe^{II} redox potential (−0.54 V vs SCE) from tripeptide [Fe^{III}(OEP)(Z-**Cys**-Leu-Gly-OMe)] (−0.61 V vs SCE). Complex **2** also indicates more positive value (−0.55 V vs SCE) than that for [Fe^{III}(OEP)(Z-**Cys**-Pro-Leu-OMe)] (−0.68 V vs SCE). We already have reported that the tetra- and tripeptides can form NH···S hydrogen bonds in the heme-thiolate model complexes, but the interaction slightly contributes to the modulation of the Fe^{III}/Fe^{II} redox potential. The α-helix model complexes indicate a large shift from the oligopeptide complexes (+0.07 to +0.13 V). Thus, α-helical conformations influence the Fe^{III}/Fe^{II} redox potential in the model complexes.

Discussion

α-Helical Conformation in the Heme-Thiolate Model Complexes. The heme-thiolate model complexes [M^{III}(OEP)-(Cys-helical peptide)] (M = Fe and Ga) form characteristic helical conformations in less polar solvent detected by ^{1}H NMR and CD spectroscopy. The helical Fe(III) complexes **1** and **2** have helical structures similar to those of the corresponding Ga(III)-substituted complexes **3** and **4** (Figure 4) just as the known oligopeptide complexes.[22] The Cys-Leu and Cys-Pro fragments indicate different conformational contributions in **1** and **2**, respectively. The helix contents of **1** (49%) and **3** (49%) are smaller than that of the corresponding thiolate anion **5** (57%). The thiolate anion **5** has the Leu-Cys-Leu-Ala fragment on the N terminus which consists of high helical tendentious residues,[25] and the lowfield shifted CysNH signal (10.14 ppm) indicates the formation of an intraresidue NH···S hydrogen bond.[40] Thus, the intraresidue NH···S hydrogen bond functions as a helix-stabilizing capping box.[49] Complexes **1** and **3** have the decreased helical contents by the coordination to the metalloporphyrin. The Cys2-Leu3-Ala4 fragment on the N terminus can make the interresidue NH···S hydrogen bond at cysteinyl sulfur atom and the amide NHs of Leu3 and Ala4 because the [Ga^{III}(OEP)(Z-**Cys**-Leu1-Gly-Leu2-OMe)] solution structure indicates the formation of the NH···S hydrogen bond of the cysteinyl sulfur atom with amide protons of Leu1 and Gly.[22] Thus, the Cys-Leu-Ala fragment of **1** and **3** intercepts α-helical NH···O═C hydrogen bond network on the N terminus formed by the interresidue NH···S hydrogen bonds.

In complexes **2** and **4**, the Pro3 following the cysteinyl residue tends to stabilize the α-helical conformation. The helical percentages of **2** (59%) and **4** (57%) are slightly larger than that of **6** (52%). The anion **6** was found to have the intraresidue NH···S hydrogen bond between CysNH and $CysS^{\gamma}$ as shown for **5** because the CysNH signal was observed at 10.65 ppm.[40] Thus, they have the intraresidue NH(Cys2)···S(Cys2) hydrogen

(49) Harper, E. T.; Rose, G. D. *Biochemistry* **1993**, *32*, 7605−7609.

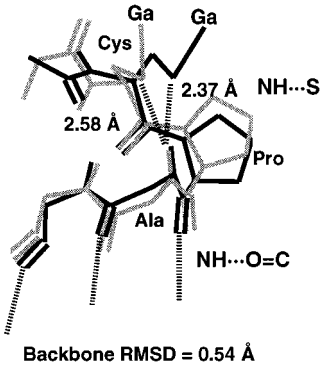

Figure 9. Superimposition of the Ga(III) complex **4** on [Ga^{III}(OEP)(Z-**Cys**-Pro-Ala-Leu-OMe)].[22] The peptide backbones of Ga(III) complex **4** and [Ga^{III}(OEP)(Z-**Cys**-Pro-Ala-Leu-OMe)] are shown as black and gray lines, respectively.

bond[41] without NH(Ala4)···S interaction because the NH(Cys2) as a favorable hydrogen bond donor is exposed to the solvent. The peptide coordination to the porphyrin thus changes the NH···S hydrogen-bonding pattern (see Figure 8). For complex **4**, the porphinato thiolate provides the NH(Ala4)···S hydrogen bond due to the steric hindrance between the OEP ring and the peptide side chains (Pro3 and Ala4) as confirmed by their higher field-shifted signals by the ring current effect. Actually, the distances of Pro3C$^{\delta}$ (4.12 Å) and Ala4C$^{\beta}$ (4.21 Å) protons from the center of the OEP ring are shorter than those of the other side chain protons. The distances of S(Cys2)−N(Cys2) and S(Cys2)−N(Ala3) are 3.81 and 3.30 Å, respectively, for **4**. The latter distance of S(Cys2)−N(Ala3) is shorter than that of [Ga^{III}(OEP)(Z-**Cys**-Pro-Ala-Leu-OMe)] (3.55 Å).[22] The shortening of the NH···S hydrogen bond is presumably caused by an increased dipole moment of the α-helical hydrogen-bonding network[50] because the backbone conformation of **4** little changes from that of [Ga^{III}(OEP)(Z-**Cys**-Pro-Ala-Leu-OMe)] shown in Figure 9. Generally, the existence of a Pro or a Cys-Pro fragment on the N terminus is favorable for an α-helix.[21,26] Actually, even [Ga^{III}(OEP)(Z-**Cys**-Pro-Ala-Leu-OMe)] has ϕ and ψ dihedral angles similar to those of an α-helix.[22] Thus, complexes **2**, **4**, and the corresponding thiolate anion **6** can maintain their similar α-helical contents by the presence of the hairpin turn of the Cys-Pro-Ala fragment on the N terminus.

Among the porphinato complexes, P-450cam and CPO, a very similar hydrogen-bonding arrangement exists between the cysteine sulfur atom and the neighboring peptide conformation. In CPO, the Cys29 sulfur is approximately 3.6 Å from each of the peptide amide groups of Ala31 and Leu32.[15] The sulfur atom, forming NH···S hydrogen bond, is located at the N terminus of the α-helix because Cys29 and Pro30 are involved in the α-helix. Thus, the sulfur atom can directly be influenced by the α-helix dipole through the NH···S hydrogen bonds. Actually, the NH···S hydrogen bond of **4** is shorter than that of the tetrapeptide complex [Ga^{III}(Z-**Cys**-Pro-Ala-Leu-OMe)].[22] Thus, the Cys-Pro-Ala-Leu of CPO fragment makes the stable α-helix and then the NH···S hydrogen bonds are influenced by the α-helix dipole. On the other hand, the dihedral angles found in the Cys357-Leu358-Gly359-Gln360 fragment at the N terminus in P-450cam deviate from an ideal α-helical conformation.[16,22] The deviation is probably caused by an enhanced flexibility of the fragment and the stronger side chain interactions in P-450 active site.[16,22] The conformational deviation was also indicated by the decrease in the helical contents of **1** and **3**. Hence, the α-helix dipole has a weaker effect on the NH···S hydrogen bonds in the Cys357-Leu358-Gly359-Gln360 fragment than those of CPO. Our investigation suggests that the nature of NH···S hydrogen bonding is regulated by the identity of invariant fragments at the N terminus and the α-helix dipole in P-450cam and CPO.

Contribution of the α-Helix Conformation to the Reactivity of P-450 and CPO. For the regulation of the Fe^{III}/Fe^{II} redox potential, we focus only on the effect of the peptide secondary structure on this potential. Several other factors that can contribute to the regulation of the redox potential are (1) the polarity of the heme environment,[51−54] (2) spin-state equilibrium which is switched by the aqua ligand at the heme coordination site,[16,55] and (3) the delicate difference in electronic structure of the heme macrocycle.[56−58] Recently, Poulos has proposed a contribution of α-helix conformation to the redox reaction.[18] We measured the Fe^{III}/Fe^{II} redox potentials for the helical peptide model complexes (Table 6). The helical peptide complexes, **1** and **2**, indicate the positive shift by 70 and 130 mV from the redox potentials of the corresponding tripeptide complexes, [Fe^{III}(OEP)(Z-**Cys**-Leu-Gly-OMe] and [Fe^{III}(OEP)(Z-**Cys**-Pro-Leu-OMe], respectively.[22] Such positive shift of the redox potential is obviously caused by α-helix conformation. Our α-helix models indicate that the α-helical conformation as well as the NH···S hydrogen bond affects the redox properties in the [Fe^{III}(OEP)(SR)] models. Furthermore, CPO model **2** (130 mV) has a larger positive shift of the Fe^{III}/Fe^{II} redox potential than that of P-450 model **1** (70 mV) since (1) the Cys-Leu-Ala- fragment of **1** partly breaks the α-helix on the N terminus and (2) the NH···S hydrogen bond in the Cys-Pro-Ala- fragment is stabilized by a favorable α-helix dipole. Therefore, the invariant fragments on the N terminus seem to be important to regulate the effect of the α-helix dipole in the native proteins. Our results indicate that the α-helical conformation coupled with NH···S hydrogen bond is one of the effects to cause positive shift of the Fe^{III}/Fe^{II} redox potential in the native folded proteins.

The high-spin 5-coordinated Fe(III) Cys-helical peptide complexes, **1** and **2**, are stable in organic solvents at 30 °C. The corresponding tetra- and tripeptide complexes containing the invariant sequences are more stable than the dipeptide or simple alkanethiolate model complexes[11,22] because the tetra- and tripeptides having P-450 and CPO invariant fragments possess lower pK_a values than those of the dipeptides in micellar solution. The solution structure of **4** indicates the intramolecular NH···S hydrogen bond which significantly contributes to the stabilization of the thiolate against the autoredox reaction because preliminary measurements of pK_a values for 2-*t*-BuCONHC$_6$H$_4$SH and 2,6-(*t*-BuCONH)$_2$C$_6$H$_3$SH indicate the shift of 1 pK_a unit per one NH···S hydrogen bond in aqueous micellar solution.[59] In addition, a pK_a value of the cysteinyl

(50) Wada, A. *Adv. Biophys.* **1976**, *9*, 1−63.
(51) Rodgers, K. K.; Sligar, S. G. *J. Am. Chem. Soc.* **1991**, *113*, 9419−9421.
(52) Kessner, R. J. *J. Am. Chem. Soc.* **1973**, *95*, 2674−2677.
(53) Gunner, M. R.; Alexov, E.; Torres, E.; Lipovaca, S. *JBIC, J. Biol. Inorg. Chem.* **1997**, *2*, 126−134.
(54) Mauk, A. G.; Moore, G. R. *JBIC, J. Biol. Inorg. Chem.* **1997**, *2*, 119−125.
(55) Fisher, M. T.; Sligar, S. G. *J. Am. Chem. Soc.* **1985**, *107*, 5018−5019.
(56) Reid, L. S.; Lim, A. R.; Mauk, A. G. *J. Am. Chem. Soc.* **1986**, *108*, 8197−8201.
(57) Koga, H.; Sagara, Y.; Yaoi, T.; Tsujimura, M.; Nakamura, K.; Sekimizu, K.; Makino, R.; Shimada, H.; Ishimura, Y.; Yura, K.; Go, M.; Ikeguchi, M.; Horiuchi, T. *FEBS Lett.* **1993**, *331*, 109−113.
(58) Unno, M.; Shimada, H.; Toba, Y.; Makino, R.; Ishimura, Y. *J. Biol. Chem.* **1996**, *271*, 17869−17874.
(59) Ueyama, N.; Yamada, Y.; Okamura, T.; Kimura, S.; Nakamura, A. *Inorg. Chem.* **1996**, *35*, 6473−6484.

thiol at the N terminus of an α-helix is smaller than a normal cysteinyl thiol pK_a.[21] Thus, the Fe(III) helical peptide complexes **1** and **2** are electronically stabilized by the contiguous α-helical conformation cooperating with the NH···S hydrogen bonds in organic solvents. Though Kortemme et al. have reported that "charge−helix interaction" contributes to the stabilizing of cysteinyl thiolate anion at the N terminus of α-helix model peptides, the net effects of electrostatic charge−helix dipole interaction and of hydrogen bonding cannot be separated experimentally.[21] Our investigation ranging from the oligopeptide complexes[22] to the helical peptide complexes has elucidated a stabilizing mechanism by invoking the contribution of the α-helix through the NH···S hydrogen bond.

Conclusion

[Fe^{III}(OEP)(Ac-L**c**XAF-LLLLL-ALFL-OMe)] {X = Leu(**1**) and (**2**)} and the Ga(III)-substituted complexes **3** and **4** were synthesized as models for P-450 and CPO. Their helical conformation depends on the character of the N-terminal fragment. The Cys-Leu-Ala fragment of **1** partly breaks the α-helix on the N terminus, but the Cys-Pro-Ala fragment of **2** cooperates with the NH···S hydrogen bond to stabilize the α-helical conformation. These conformations influence the Fe^{III}/Fe^{II} redox reaction. The redox potential of **1** indicates only a shift of 70 mV from the value of [Fe(OEP)(Z-**Cys**-Leu-Gly-OMe)]. On the other hand, complex **2** shows a larger shift of 130 mV of Fe^{III}/Fe^{II} redox potential from that of [Fe(OEP)(Z-**Cys**-Leu-Gly-OMe)]. The large shift is caused by the α-helical dipole coupled with the NH···S hydrogen bond. Our investigation now experimentally clarified that the α-helix cooperating with the NH···S hydrogen bond formed by the invariant sequences induces the positively shifted redox potential and contributes to thermal stability of high-spin 5-coordinated Fe(III) thiolate state. Further model investigations including effects of the specific polypeptide environment are obviously necessary to solve the mechanism(s) of the enzymatic reactions of heme-thiolate proteins.

Experimental Section

Materials. All operations were performed under an argon atmosphere. Dichloromethane, and all other solvents were purified by distillation before use. M^{III}(OEP)(OMe) (M = Fe and Ga) was prepared by the literature methods.[60,61]

Preparation of Ac-LCXAF-LLLLL-ALFL-OMe (X = Leu and Pro). The peptides used in this paper were assembled by using an automated solid-phase peptide synthesizer (Applied Biosystems Inc., Model 430A). The final protected peptide resin was treated with anhydrous hydrogen fluoride in the presence of 5% *p*-cresol at −2 °C for 60 min. The crude peptide carboxylic acid was treated with 1 N HCl/dioxane in the solution of MeOH/methylene chloride to obtain the corresponding methyl ester. The final methyl ester derivatives were purified by the recrystallization from chloroform/hexane or methanol/hexane. Homogeneities of the final products were confirmed by analytical HPLC and amino acid analysis.

Synthesis of [Fe^{III}(OEP)(Ac-LcLAF-LLLLL-ALFL-OMe)] (1). A CH_2Cl_2 (1 mL) solution of [Fe^{III}(OEP)(OMe)] (3.8 mg, 6.2×10^{-3} mmol) was added to Ac-LCLAF-LLLLL-ALFL-OMe (10.1 mg, 6.2×10^{-3} mmol) in CH_2Cl_2 (3 mL). The solution was stirred for 15 min at ambient temperature. The solvent was removed under reduced pressure to give a deep red powder. MS (ESI) calcd (found) *m*/*e*: (**1** + H^+), 2220.3 (2220.3). 400-MHz ^{1}H NMR (CD_2Cl_2 at 30 °C, δ ppm): −45.0 [*meso*(OEP)], 40.1 [α-CH_2(OEP)], 39.7 [α-CH_2(OEP)], 6.3 [β-CH_2(OEP)].

Synthesis of [Fe^{III}(OEP)(Ac-LcPAF-LLLLL-ALFL-OMe)] (2). This complex was synthesized by the same ligand exchange reaction as used for **1** to give a deep red powder. MS (ESI) calcd (found) *m*/*e*: (**2** + H^+), 2204.3 (2204.1). 400-MHz ^{1}H NMR (CD_2Cl_2 at 30 °C, δ ppm): −43.9 [*meso*(OEP)], 42.9 [α-CH_2(OEP)], 40.4 [α-CH_2(OEP)], 6.7 [β-CH_2(OEP)].

Synthesis of [Ga^{III}(OEP)(Ac-LcXAF-LLLLL-ALFL-OMe)] {X = Leu (3) and Pro (4)}. The titled complexes were prepared by a ligand-exchange reaction as described in a previous paper.[22] [Ga^{III}-(OEP)(Ac-LcLAF-LLLLL-ALFL-OMe)] **(3).** UV−vis (dichloromethane): 350 nm (38 000), 412 nm (235 000), 537 nm (18 200), and 574 nm (20 600). MS (ESI) calcd (found) *m*/*e*: (**3** + H^+), 2233.3 (2234.5). 400-MHz ^{1}H NMR ($CDCl_3$ at 27 °C, δ ppm): 10.36 [*meso*(OEP)], 4.16 [α-CH_2(OEP)], 4.26 [α-CH_2(OEP)], 1.94 [β-CH_2-(OEP)], −1.15 (CysC^βH1), −3.20 (CysC^βH2). [Ga^{III}(OEP)(Ac-LcPAF-LLLLL-ALFL-OMe)] **(4).** UV−vis (dichloromethane): 349 nm (40 000), 411 nm (263 000), 536 nm (20 000), 573 nm (24 000). MS (ESI) calcd (found) *m*/*e*: (**4** + H^+), 2217.3 (2218.2).

Preparation of (Et_2N){Ac-LC(S^-)XAF-LLLLL-ALFL-OMe} {X = Leu(5) and Pro (6)}. These cysteinyl thiolate anion peptides were prepared by the reported method.[41] The dichloromethane solution (0.45 mL) of (Et_4N)(S-*t*-Bu) (0.35 mg, 1.6×10^{-3} mmol) was added to a solution of Ac-LCLAF-LLLLL-ALFL-OMe (2.59 mg, 1.59×10^{-3} mmol) in 1 mL of CH_2Cl_2. **6** was also prepared by the same procedure.

Physical Measurements. UV−visible spectra were recorded on a Shimadzu UV3100PC. Circular dichroism (CD) and magnetic circular dichroism (MCD) measurements were recorded on a Jasco J-720w spectropolarimeter equipped with an electromagnet operated at 1.5 T. These measurements were carried out using a 0.1- or 0.01-cm cell path. The measurements of cyclic voltammograms in dichloromethane solution were carried out on a BAS 100 B/W instrument with a three-electrode system: a glassy carbon working electrode, a Pt-wire auxiliary electrode, and a saturated calomel electrode (SCE). The scan rate was 100 mV/s. The concentration of sample was 2.0 mM, containing 200 mM *n*-Bu_4NClO_4 as a supporting electrolyte. Potentials were determined at room temperature vs a saturated calomel electrode (SCE) as a reference. Mass spectrometric analyses were performed on a Finniganmat LCQ-MS instrument in acetonitrile/dichloromethane.

NMR Spectroscopy. NMR spectra were acquired in $CDCl_3$ on a Varian Unityplus 600-MHz spectrometer. Tetramethylsilane (TMS) was used as the internal reference for proton resonances, and 2.0 mM solutions were used for all conformational analyses at 27 °C. Variable-temperature NMR measurements were performed on a JEOL JNM-LA 500 NMR spectrometer for **5** and **6**. The temperature dependence of the amide proton of **4** signals was assigned by variable-temperature DQF-COSY[62] experiments. In one run, measurements were made in the range 228−303 K, and then the temperature was decreased in 15 K intervals. The sample temperatures were controlled with the variable-temperature unit of the instrument.

Complete proton resonance assignments were made using DQF-COSY and TOCSY[63,64] experiments. ROESY[65,66] experiments were used to extract interproton distances. All 2D spectra were acquired in the phase-sensitive mode. DQF-COSY, TOCSY, and ROESY spectra were recorded with 9000−9600-Hz spectral width in both dimensions and 1024 data points in *f*2 and 512 data points in *f*1 with eight scans at each increment. The ROESY spectra were recorded with five different mixing times, 50, 100, 150, 200, and 250 ms, to generate ROE built-up curves. The ROE intensities obtained at a 200-ms mixing time were found to be in the middle of the linear curves. Therefore, interproton distances of the gallium complexes and the cysteinyl thiolate anions were deduced from the ROESY experiments carried out at a 200-ms mixing time. Assigned cross-peaks were converted into distance restraints by volume integration of the ROESY spectrum,

(60) Hatano, K.; Uno, T. *Bull. Chem. Soc. Jpn.* **1990**, *63*, 1825−1827.
(61) Okamura, T.; Nishikawa, N.; Ueyama, N.; Nakamura, A. *Chem. Lett.* **1998**, 199.
(62) Piantini, V.; Sorensen, O.; Ernst, R. R. *J. Am. Chem. Soc.* **1982**, *104*, 6800−6801.
(63) Bax, A.; Davis, D. G. *J. Magn. Reson.* **1985**, *65*, 355−360.
(64) Braunschweiler, L.; Ernst, R. R. *J. Magn. Reson.* **1983**, *53*, 521−528.
(65) Bothner-By, A. A.; Stephens, R. L.; Lee, J.-M.; Warren, C. D.; Jeanloz, R. W. *J. Am. Chem. Soc.* **1984**, *106*, 811−813.
(66) Rance, M. J. *J. Magn. Reson.* **1987**, *74*, 557−564.

taking the most intense peak between diastereotopic protons as a reference of 1.80 Å. The distances were classified into three ranges, 1.8−2.5, 1.8−3.5, and 1.8−5.0 Å, corresponding to strong, medium, and weak ROEs. Distances to methyl and methylene protons, not stereospecifically assigned, were calculated with respect to the average position of these protons (pseudo-atom representation), and the appropriate corrections to the upper limits of the corresponding restraints were applied. The two-dimensional data sets were processed with the program FELIX ver. 95.0 (Molecular Simulations Inc., San Diego, CA) on an SGI INDIGO2 workstation. The data were zero filled to give a final matrix of 2K × 2K. A squared sine-bell window function was used for the ROESY experiments.

Computational Procedure. All of the simulations of peptide parts for Ga(III) model complex **4** were carried out in vacuo using the CVFF[67] force field as implemented in Discover (Molecular Simulations Inc., San Diego, CA). All of the calculations used a distance-dependent macroscopic dielectric constant of 1**r* and infinite cutoff nonbonded interactions to partially compensate for the lack of explicit solvent. Distance restraints were incorporated into all of the energy calculations using a skewed biharmonic function (Molecular Simulations Inc.). A force constant of 50 kcal mol^{-1} Å^{-1} for k_{upp} and k_{low} and a maximum force of 1000 kcal mol^{-1} Å^{-2} were used. Backbone NH(i)···O═C(i+4) (i = 1−10) hydrogen bonds were also introduced as restraints using a force constant of 100 kcal mol^{-1} Å^{-1} to reproduce the proportionality found for the chemical shift temperature coefficient values[68] in the absence of a hydrogen bond constraint between NH of Ala4 and Sγ of Cys2. The model was initially minimized using a steepest descent to a gradient of 0.01 kcal mol^{-1} Å^{-1} for the maximum iteration of 100. The structure was further minimized to a maximum gradient of 0.01 kcal mol^{-1} Å^{-1} using a conjugate gradient for the maximum iteration of 500. Restrained molecular dynamics (rMD) were performed typically at 1000 K on the minimized structure using step size of 1 fs for the integration of Newton's equation (*Verlet leapfrog* algorithm[69]). After equilibration for an initial 1 ps by direct scaling of the velocities, the system was coupled to a temperature bath at 1000 K for 50 ps, gradually increasing the scaling factors of restraints from 10^{-6} to 1 and that of covalent and nonbonded terms from 0.001 to 1. These were then subjected to annealing by decreasing of the temperature during 10 ps via bath coupling to 300 K. Each resulting annealed structure was then minimized using the procedure above to give 50 final frames. The soft-core potential for the repulsion between atoms was used through the beginning minimization, dynamics, and the minimization after the dynamics followed by the minimization using the Lennard-Jones potential. Among all of these structures, only those with no root-mean-square (rms) deviation larger than 0.4 Å for backbone heavy atom from the lowest ROE violation structure were kept and used for the structural comparisons. Refinement of the averaged structures among them was achieved by preliminary molecular mechanics. Molecular modeling experiments of the gallium complexes employed the reported procedure.[22] The averaged peptide structure of **4** served as the initial conformation of the model complexes.

Acknowledgment. We are grateful for financial supports by JSPS Fellowships (to T.U.; No. 2691(1995-1998)) and by a Grant-in-Aid for Specially Promoted Research from the Ministry of Education, Science and Culture (to A.N.; No. 06101004). We also thank Dr. Kenichi Lee and Mr. Hiroshi Adachi of Graduate School of Science, Osaka University, for their assistance with the NMR and ESI-MS measurements, respectively. We acknowledge Professor Sumio Kaizaki, Department of Chemistry, Graduate School of Science, Osaka University, for circular dichroism and magnetic circular dichroism measurements.

Supporting Information Available: Two tables and two figures showing NMR chemical shifts and summary of ROEs observed in the ROESY spectra of **2** and **3** (4 pages, print/PDF). See any current masthead page for ordering information and Internet access instructions.

JA980016D

(67) Hagler, A. T.; Hulter, E.; Lifson, S. *J. Am. Chem. Soc.* **1974**, *96*, 5319−5327.

(68) Kessler, H. *Angew. Chem., Int. Ed. Engl.* **1982**, *21*, 512−523.

(69) Van Gunsteren, W. F.; Berendsen, H. J. C. *Mol. Phys.* **1977**, *34*, 1311−1327.

(70) Schlotz, J. M.; Qian, H.; York, E. J.; Stewart, J. M.; Baldwin, R. L. *Biopolymers* **1991**, *31*, 1463−1470.

(71) Chakrabartty, A.; Schellman, J. A.; Baldwin, R. L. *Nature* **1991**, *351*, 586−588.